Biophysical Chemistry 184 (2013) 37–43

Contents lists available at ScienceDirect

Biophysical Chemistry

journal homepage: http://www.elsevier.com/locate/biophyschem

Membrane protein reconstitution into liposomes guided by dual-color fluorescence cross-correlation spectroscopy

Peter Simeonov [a,1], Stefan Werner [b,1], Caroline Haupt [a,1], Mikio Tanabe [a,*], Kirsten Bacia [b,**]

[a] Membrane Protein Biochemistry, HALOmem, University of Halle, Kurt-Mothes-Str. 3, D-06120 Halle (Saale), Germany
[b] Biophysical Chemistry of Membranes, HALOmem, University of Halle, Kurt-Mothes-Str. 3, D-06120 Halle (Saale), Germany

HIGHLIGHTS

- Reconstitution into liposomes facilitates studies of membrane protein function.
- We show that FCCS tests protein and lipid co-localization in diffusing particles.
- FCCS can be used to guide a membrane protein reconstitution process.
- The multidrug resistance transporter NorA was functionally reconstituted.

GRAPHICAL ABSTRACT

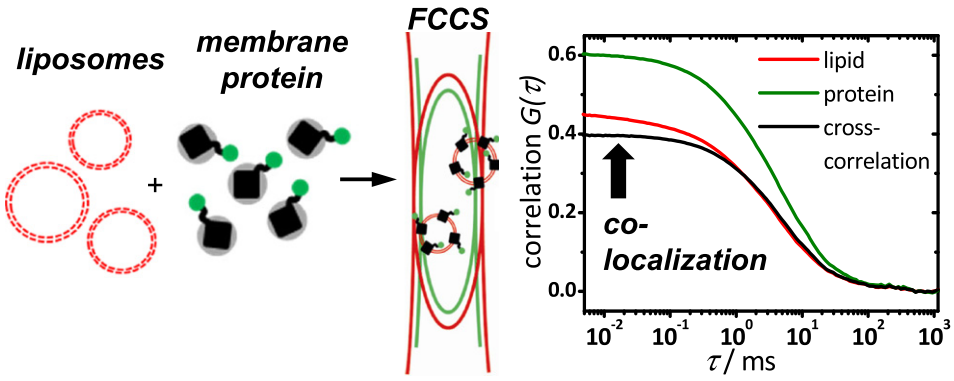

ARTICLE INFO

Article history:
Received 1 July 2013
Received in revised form 8 August 2013
Accepted 9 August 2013
Available online 20 August 2013

Keywords:
Membrane protein reconstitution
Proteoliposome
Multidrug resistance transporter
NorA
Dual-color fluorescence cross-correlation spectroscopy (FCCS)
Fluorescence correlation spectroscopy (FCS)

ABSTRACT

Proteoliposomes represent nanoscale assemblies of indispensable value for studying membrane proteins in general and membrane transporters in particular. Since no universal protocol exists, conditions for proteoliposome formation must be determined on a case-by-case basis. This process will be significantly expedited if the size and composition of the assemblies can be analyzed in a single step using only microliters of sample. Here we show that dual-color fluorescence cross-correlation spectroscopy (FCCS) is of great value for optimizing the reconstitution process, because it distinguishes micelles, liposomes and aggregates in heterogeneous mixtures and permits direct monitoring of the co-localization of proteins and lipids in the diffusing assemblies. As proof-of-principle, liposomes containing the functional multidrug resistance transporter NorA from *Staphylococcus aureus* were prepared, demonstrating that FCCS is an excellent tool to guide the development of reconstitution protocols.

1. Introduction

Membrane proteins play vital roles in all organisms ranging from bacteria to higher eukaryotes. From an analytical point of view, a high quality reconstitution of a purified membrane protein into a lipid bilayer is a prerequisite for various biochemical and biophysical studies of membrane protein function. The need for reconstitution of the protein

* Corresponding author. Tel.: +49 345 55 24923.
** Corresponding author. Tel.: +49 345 55 24924; fax: +49 345 55 27408.
E-mail addresses: mt@halomem.de (M. Tanabe), kb@halomem.de (K. Bacia).
[1] These authors contributed equally to this work.

0301-4622
http://dx.doi.org/10.1016/j.bpc.2013.08.003

into a lipid bilayer is particularly obvious for membrane transporters, because they – unlike for instance membrane receptors or enzymes – are only able to perform their transport function in the membrane-embedded form. Membrane transporters are universally found, integral membrane proteins that translocate substances actively (against an electrochemical gradient) or passively (by facilitated diffusion) across membranes [1].

Phospholipid vesicles (liposomes) have been shown to be an excellent tool for investigating the function of membrane transporters. Proteoliposomes consist of a self-closed phospholipid bilayer, into which the purified membrane transporter is incorporated [2]. Several methods are employed to insert the protein into the liposome, among which the detergent-mediated pathway is the most prominent one [3–5]. The membrane transporter, which is solubilized by detergent during purification, can be directly mixed with detergent-destabilized liposomes to form mixed phospholipid–protein–detergent complexes. Removal of the detergent forces the protein to associate with the phospholipid membrane, resulting in the desired proteoliposomes (Fig. 1A). The destabilization of the preformed liposomes by the addition of detergent and the subsequent removal of the detergent are critical steps during the reconstitution procedure.

Despite the usefulness and versatility of detergent-mediated reconstitution, optimizing the reconstitution conditions to obtain a homogeneous proteoliposome preparation with functionally integrated protein, with the desired protein-to-lipid ratio, and with the desired size and liposome integrity remains a major challenge. Several experimental techniques are employed for supporting detergent-mediated reconstitution [6,7]. Due to their ease of use, turbidimetry and light scattering are routinely performed. A marked decrease in the turbidity or light scattering signal indicates membrane solubilization on the conversion of liposomes to micelles [4,8,9]. Nuclear magnetic resonance (NMR) spectroscopy is best suited to analyze the starting point of the solubilization process [10–13]: as opposed to the broadened NMR signal of a phospholipid bilayer, a narrow isotropic signal is generated when micelles appear, making the vesicle–micelle transition easily detectable. One major disadvantage of NMR spectroscopy is its low sensitivity and hence the necessity for large amounts of highly concentrated samples. Other methods for analyzing membrane solubilization comprise infrared (IR) spectroscopy [14,15], fluorescence spectroscopy [6,16,17] including fluorescence energy transfer [18,19], isothermal titration calorimetry (ITC) [20,21], electron spin resonance (ESR) [22], X-ray diffraction [23], atomic force microscopy (AFM) [24,25] and electron microscopy (EM) [26–28].

One drawback with several techniques used to assist with membrane protein reconstitution is that they permit to analyze the solubilization of the liposomes but not the reconstitution of the protein itself. Another drawback with many techniques is that sample-averaged parameters are obtained which are not informative about potential sample inhomogeneity resulting from the solubilization and assembly processes. In particular, IR spectroscopy, fluorescence spectroscopy and ITC are limited to bulk observations. Although AFM and EM permit visualization of individual particles, the results can be biased, as some

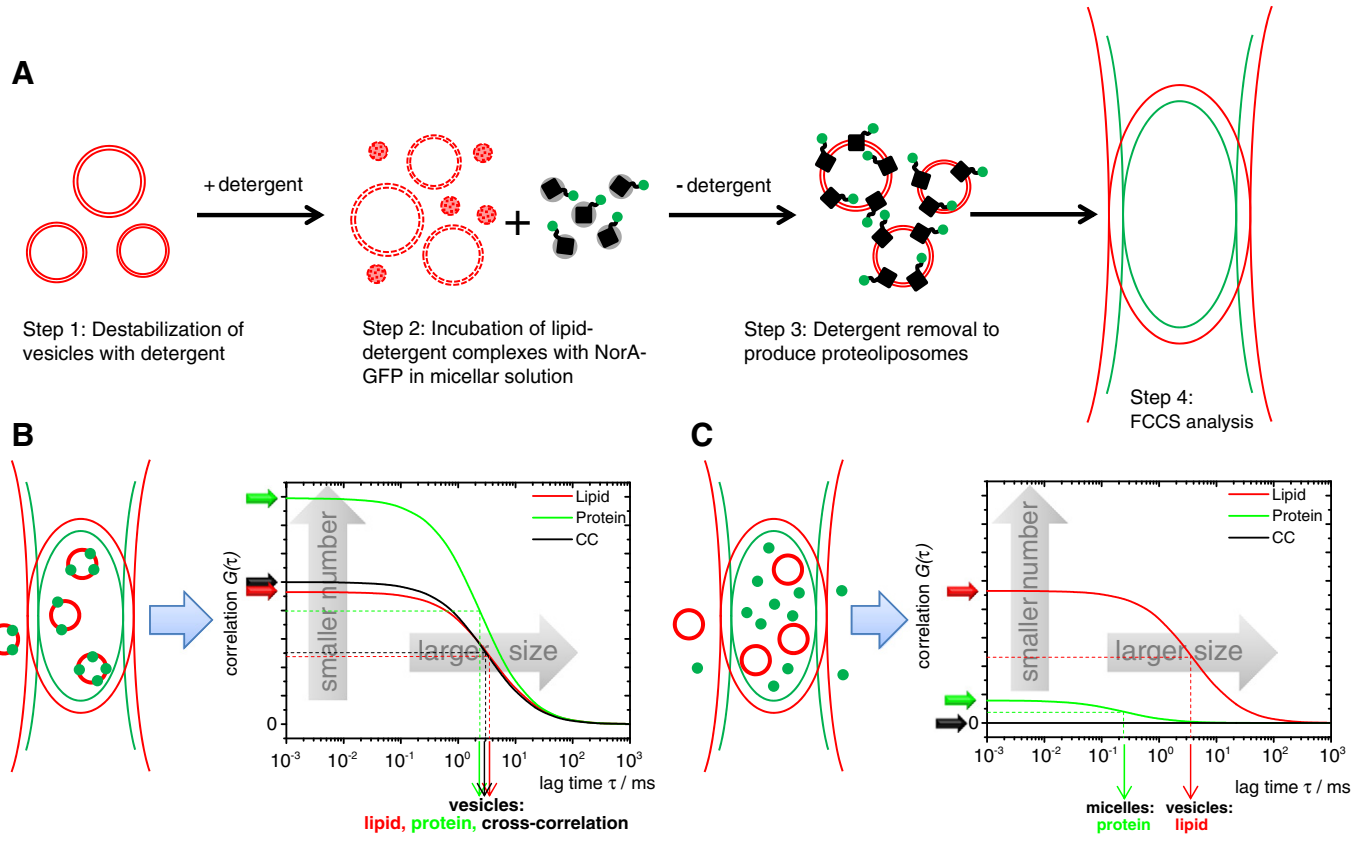

Fig. 1. (A) Schematic overview of the reconstitution procedure. Destabilization of liposomes with detergent yields detergent-containing liposomes and/or lipid-containing micelles (Step 1). Detergent-solubilized protein is added (Step 2). After detergent removal, FCCS is used to assess the particle numbers, particle types, relative particle contributions and the relative co-localization of protein and lipid (Steps 3 & 4). (B) Simulated auto- and cross-correlation curves for an ideal proteoliposome sample (concentrations of red and green particles are identical). The red autocorrelation amplitude is lower than the green one, because the red detection volume is larger. The cross-correlation amplitude is in between the two autocorrelation amplitudes, demonstrating maximal co-localization. All three curves exhibit a diffusion time typical of liposomal particles. (C) Simulated dual-color FCCS curves representing separate diffusion of liposomes (red) and protein (green). Total concentrations of red and green dye are the same as in panel B. As the protein molecules diffuse as individual entities, the number of green particles is larger than in panel B, causing a lower autocorrelation amplitude. The cross-correlation amplitude is zero, demonstrating the absence of co-localization between protein and liposomes. Lipid particles exhibit a diffusion time typical of liposomes, whereas protein molecules exhibit a diffusion time typical of micelles.

types of particles may be less well preserved during sample preparation or harder to visualize. It is therefore desirable to complement the current repertoire of techniques for monitoring and optimizing membrane protein reconstitution with alternatives that demand only small amounts of sample and short measurement times, while providing insight into sample heterogeneity.

Here we introduce fluorescence correlation spectroscopy (FCS) as a complementary approach for monitoring both the membrane solubilization and the reconstitution steps with just one technique (Fig. 1A). In contrast to turbidimetry, FCS allows the distinction and simultaneous analysis of different types of particles (micelles, liposomes, aggregates) based on their characteristic diffusion coefficients. FCS is a highly sensitive method that observes single diffusing fluorescent particles and requires only small sample volumes and concentrations [29]. In dual-color fluorescence cross-correlation spectroscopy (FCCS), an extension of FCS, the fluorescence fluctuations arising from the diffusion of two distinct fluorophores are analyzed [30]. In the current application, we exploit the cross-correlation between green-labeled membrane protein and red-labeled liposomes as a test for the concomitant movement of protein and liposomes on the single particle level. The relative cross-correlation amplitude hence provides a straight-forward measure for the formation of proteoliposomes (Fig. 1B,C).

We have used the endogenous multidrug resistance (MDR) transporter NorA from *Staphylococcus aureus* to demonstrate the optimization of the reconstitution process by using FCS and dual-color FCCS. NorA is of large clinical importance because of an increasing number of methicillin-resistant *S. aureus* (MRSA) infections, as NorA is capable of expelling a number of antibiotics used to combat MRSA infection [31]. NorA belongs to the Major Facilitator Superfamily (MFS), which is the largest family of MDR transporters. It consists of 12 putative transmembrane segments and is located in the cytoplasmic membrane [31,32]. Besides the fluoroquinolone antibiotic resistance that first allowed the identification of NorA [31], NorA confers resistance to a broad range of compounds including rhodamine, ethidium bromide, puromycin, chloramphenicol and pentamidine [33,34]. The active efflux of these drugs and organic compounds is coupled to the proton gradient across the membrane. It was previously shown that NorA also transports the dye Hoechst 33342 both in everted membrane vesicles and when reconstituted into liposomes [35]. We therefore chose NorA as a promising target for establishing an FCCS-guided membrane protein reconstitution approach.

2. Material and methods

2.1. NorA recombinant expression and purification

The *norA* gene was cloned into the pWaldo-eGFP vector [36–38], transformed into *Escherichia coli* C43 (*DE3*) and recombinantly expressed in Terrific Broth (TB) medium. The membrane fraction was subsequently solubilized with 1% n-dodecyl-β-D-maltopyranoside (DDM; Affymetrix Anatrace) and the NorA-eGFP fusion protein (referred to as NorA-GFP) was purified by immobilized metal ion affinity chromatography (IMAC). See Supplementary data for details.

2.2. Liposome preparation and destabilization

Liposome preparation and destabilization were performed based on Knol et al. [39] with small modifications. Briefly, a mixture of *E. coli* polar lipid crude extract (44 μL of 25 mg/mL; Avanti Polar Lipids) and the fluorescent lipid analog DiD-C_{18} (2.5 μL of a 3 mM stock solution; 1,1′-dioctadecyl-3,3,3′,3′-tetramethylindodicarbocyanine perchlorate; Invitrogen) was prepared in chloroform and dried under nitrogen for at least 1 h. The lipid film was hydrated in reconstitution buffer (1 mL, 20 mM KH_2PO_4 (pH 7.0), 100 mM potassium acetate, 2 mM $MgSO_4$) and incubated for 1 h (final lipid concentration 1.1 mg/mL). The resulting liposomes were extruded 21 times through polycarbonate filters with a pore size of 100 nm using a Mini-Extruder (Avanti Polar Lipids) according to the manufacturer's protocol. Liposome size was analyzed by dynamic light scattering (Malvern Zetasizer Nano S). Liposomes were stored at 4 °C. Prior to detergent destabilization, liposomes were diluted in extrusion buffer (0.22 mg/mL). Liposome destabilization was achieved by the stepwise addition of Triton X-100 (1 μL 1% (v/v) per step) to 100 μL of the liposome suspension [40]. The detergent Triton X-100 (critical micelle concentration ≈ 0.2 mM) was obtained from Sigma–Aldrich. Destabilization was monitored by following the turbidity at 460 and 540 nm [4] using a Tecan infinite M200Pro spectrometer (Tecan instruments) and by measuring diffusion times and particle brightnesses by FCS (see details below).

2.3. Functional reconstitution of NorA-GFP into proteoliposomes

NorA-GFP was reconstituted into liposomes based on a published protocol [35], which was modified using the information from the dual-color FCCS results. Destabilized liposomes (200 μL) were mixed with concentrated NorA-GFP (30 μL of ~10 mg/mL). After a 30 min incubation at room temperature, small amounts (4–10 beads) of polystyrene Bio-Beads SM-2 (Bio-RAD) were added [41]. The addition of Bio-Beads was repeated after 2 h and after 4 h. Overnight storage was at 4 °C. The next day, three more additions of Bio-Beads were repeated at intervals of 2 h at room temperature. Prior to FCS and transport analysis, the proteoliposome solution was centrifuged to remove large aggregates (60 s at 10,000 ×*g*). For FCS analysis, an aliquot was diluted 10-fold into reconstitution buffer and pipetted onto a glass coverslip coated with bovine serum albumin (final volume 20 μL). The step-by-step improvement of the reconstitution protocol is shown in the Results and discussion section.

2.4. Dual-color FCCS

Dual-color FCCS was conducted on a ConfoCor3/LSM710 setup (Carl Zeiss), using a C-Apochromat 40×/1.2 N.A. water immersion objective. The green fluorescent chromophores (eGFP, Alexa Fluor 488) were excited by the 488 nm line of an argon ion laser, the red fluorescent dyes (DiD-C_{18}, Alexa Fluor 633) by a 633 nm helium–neon laser. Absorption and emission maxima of eGFP are located at 490 nm and 509 nm, respectively; absorption and emission maxima of DiD-C_{18} in liposomes are at 652 nm and 670 nm, respectively (absorption data measured on a Tecan Infinite M200Pro, fluorescence emission on a Horiba Fluoromax-2 instrument). For dual-color FCCS on the ConfoCor3/LSM710 setup, the emission signals were split with a 635 nm dichroic mirror. A 505 to 610 nm bandpass emission filter was used in the green channel and a 655 nm longpass emission filter in the red channel. Count rates in each channel were adjusted to minimize cross-talk and avoid detector saturation by tuning the excitation intensities with an acousto-optical tunable filter. The red observation volume in this setup is larger than the green observation volume. Hence an optimally reconstituted sample that consists only of double-labeled particles shows a green autocorrelation amplitude that is higher than the red one (see simulation in Fig. 1B).

Using calibration measurements from dyes of known diffusion coefficients in water (Alexa Fluor 488 hydrazide [42]; Alexa Fluor 633 hydrazide [43]; both dyes from Invitrogen) the structure parameter $S = z_o / \omega_o$, i.e. the ratio of the axial to lateral radii of the detection volumes, was determined to be $S = 6$ and the lateral radii of the detection volumes to be $\omega_o = 0.265$ μm (red channel) and $\omega_o = 0.212$ μm (green channel). The relationship between the diffusion coefficient D_i of a particle and the measured diffusion time $\tau_{\mathrm{diff},i}$ is given by

$$D_i = \frac{\omega_o^2}{4\tau_{\mathrm{diff},i}}. \quad (1)$$

2.5. Curve fitting and analysis of dual-color FCCS measurements

FCS curves of the reconstitution samples were fitted with model equations containing one or two freely diffusing species and one blinking term:

$$G(\tau) = G(0)\left[1 + \frac{T\, e^{-\frac{\tau}{\tau_{trip}}}}{1-T}\right]\sum_i \frac{F_i}{\left(1+\frac{\tau}{\tau_{diff,i}}\right)\sqrt{1+\frac{\tau}{S^2\tau_{diff,i}}}} \quad (2)$$

$\tau_{diff,i}$ ≡ diffusion time of species i; F_i ≡ apparent fraction of species i; S ≡ structure parameter; T ≡ fraction of particles in the triplet or other dark state; and τ_{trip} ≡ triplet or other dark state relaxation time.

The same model equation but without the blinking term was used for the cross-correlation:

$$G_x(\tau) = G_x(0)\sum_i \frac{F_i}{\left(1+\frac{\tau}{\tau_{diff,i}}\right)\sqrt{1+\frac{\tau}{S^2\tau_{diff,i}}}}. \quad (3)$$

The structure parameter S was set to the fixed value of 6 obtained during the calibration measurements. The fits were conducted with the ZEN 2009 software (Carl Zeiss Jena).

The measured apparent fractions F_i are related to the concentrations, weighted with the square of the brightnesses:

$$G(0) = \frac{1}{V_{eff}}\frac{\sum_i \eta_i^2 c_i}{\left[\sum_i \eta_i c_i\right]^2} \quad (4)$$

$G(0)$ ≡ autocorrelation amplitude; V_{eff} ≡ effective observation volume; η_i ≡ molecular brightness of species i; and c_i ≡ concentration of species i.

2.6. Hoechst 33342 transport assay with NorA-GFP proteoliposomes

A transport assay using the dye 2'-(4-ethoxyphenyl)-5-(4-methyl-1-piperazinyl)-2,5'-bi-1H-benzimidazole (Hoechst 33342) was performed according to Yu et al. [35]. The proton gradient was generated by diluting the proteoliposomes (containing 20 mM KH_2PO_4 (pH 7.0), 100 mM potassium acetate, 2 mM $MgSO_4$) 20-fold into 20 mM KH_2PO_4 (pH 7.0), 50 mM potassium sulfate, 2 mM $MgSO_4$. Fluorescence quenching was measured using a Horiba FluoroMax SPEX 3 spectrofluorimeter (excitation at 355 nm, emission at 457 nm, slit widths of 5 nm and 8 nm). Tetraphenylphosphonium bromide (TPP) was added to study the effect of this reagent on Hoechst 33342 transport. The time course of fluorescence intensity changes was measured after the addition of Hoechst 33342.

3. Results and discussion

3.1. Liposome destabilization for protein reconstitution

To facilitate membrane protein insertion, liposomes are usually destabilized by the addition of detergents. We first followed the transition from liposomes to micelles as a function of Triton X-100 concentration using a standard turbidity assay [4]. The turbidity plot allows the distinction of three stages (Fig. 2A). During the first stage, detergent partitions into the vesicle bilayer until saturation is reached (detergent concentration $[D]_{sat} \approx 0.9$ mM). During stage II, further addition of detergent leads to a decreasing number of detergent-saturated vesicles, which coexist with a growing number of lipid-saturated mixed micelles. This stage is evidenced by a gradual decrease in turbidity. Finally, at a detergent concentration of $[D]_{sol} \approx 2.2$ mM, solubilization is complete, i.e. the solution contains only mixed micelles, and the turbidity enters a plateau region (stage III).

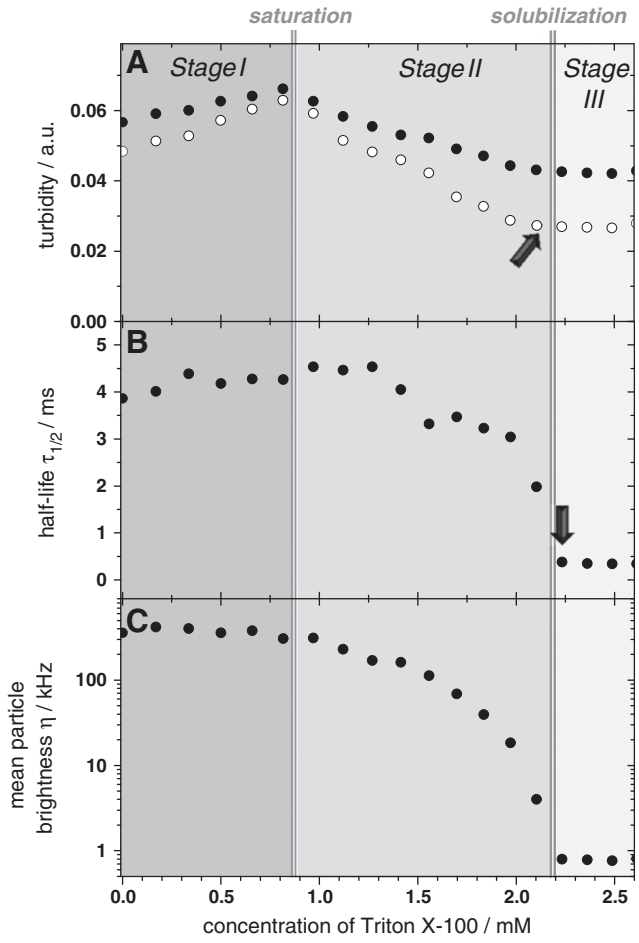

Fig. 2. Destabilization of phospholipid vesicles with Triton X-100, monitored by turbidity and by FCS. (A) As a measure of turbidity, optical density at 540 nm (filled circles) and at 460 nm (open circles) is plotted versus detergent concentration. Turbidity most easily identifies the saturation limit, i.e. the onset of solubilization at ≈0.9 mM Triton X-100. (B) FCS correlation curve half-lives are more sensitive to the completion of solubilization than turbidity (arrows). A sharp drop in the diffusion time occurs as the last remaining liposomes are micellized at ≈2.2 mM Triton X-100 (arrow). (C) The mean particle brightness (the product of the mean fluorescence count rate and the diffusional correlation amplitude) is also highly sensitive to the completion of solubilization.

In some instances, the use of turbidity data alone for revealing the course of solubilization can be misleading, because saturation and solubilization points may be obscured, as detergent-resistant membranes are encountered [16,44] or phase separation due to micelle–micelle interactions occurs. As a consequence, turbidity may increase and conceal the expected decrease during solubilization [12,45]. In preparation for the development of an FCCS-based reconstitution assay, we therefore asked if the course of solubilization could also be monitored directly using the FCS setup.

The half-life of the FCS correlation curve $G(\tau)$ as an estimate of the mean diffusion time τ_{diff} (Fig. 2B) and the mean particle brightness (Fig. 2C) can serve as a complementary way of assessing stages I, II and III of solubilization. We note that turbidity allows a more precise determination of the point of saturation (based on the change from positive to negative slope), while FCS is more precise at determining the point of complete solubilization. In the turbidity plot, the completion of solubilization can only be estimated roughly from a gradual change in the slope (Fig. 2A, arrow), whereas the FCS measurements show a prominent shift to a single component of $\tau_{diff} \approx 0.38$ ms (particle diameter $2R_H = 10$ nm, micelles) precisely at the point where no more liposomes are present ($\tau_{diff} \approx 3.5\ldots4.6$ ms, particle diameter $2R_H = 90\ldots120$ nm) (Fig. 2B, arrow).

Using turbidity and FCS, the course of liposome destabilization by the detergent can be monitored and specific conditions chosen for membrane protein reconstitution attempts.

3.2. Dual-color fluorescence cross-correlation spectroscopy

Dual-color FCCS analyzes the dynamic co-localization of two differently labeled (e.g. green and red) fluorescent particles or molecules. We have exploited the co-localization information from the amplitudes of the correlation curves along with the particle size information from the decays to rapidly assess the incorporation of a green fluorescently tagged transmembrane protein (NorA-GFP) into red fluorescent (DiD-labeled) phospholipid vesicles.

A positive cross-correlation amplitude arises when green and red fluorescent chromophores diffuse together through the observation volume. A high amplitude of the cross-correlation curve compared to the autocorrelation curves indicates a large proportion of double-labeled particles, indicating a successful reconstitution of the transmembrane protein into the liposomes (Fig. 1B). A low cross-correlation amplitude signifies a poor reconstitution yield (Fig. 1C). The cross-correlation and autocorrelation curves can also be analyzed with respect to the sizes and apparent relative concentrations of particles, allowing a distinction between micelles, vesicles and aggregates. In FCS, as demonstrated by Eq. (4), brighter particles (liposomes and aggregates that carry several GFP-tagged protein molecules) contribute more strongly to the measured fractions than dim particles (such as micelles that carry a single GFP).

3.3. Optimizing the reconstitution of NorA-GFP

NorA-GFP was successfully expressed and purified by a single step IMAC procedure (Fig. S1). For the reconstitution, we first tested the use of fully solubilized lipid (2.6 mM Triton, mixed micelles, see Fig. 2) as the starting material, to which the solubilized NorA-GFP and the Bio-Beads (for detergent removal) were added. Fig. 3A shows that this approach resulted in a poor reconstitution yield. Detergent removal was sufficiently effective to convert the mixed detergent–lipid micelles into liposomes, as evidenced by the single component fit of the red autocorrelation curve with a diffusion time typical for liposomes [τ_{diff} = 2.3 ms, $2R_H$ = 60 nm]. However, the low amplitude of the green autocorrelation points to a large number of particles, denoting non-reconstituted protein. Moreover, the green autocorrelation curve requires a two-component fit model (33% of τ_{diff} = 0.16 ms [micelles] and 67% of τ_{diff} = 2.2 ms [liposomes]), showing that a large part of the protein is still in micelles. The cross-correlation corroborates this interpretation: The cross-correlation amplitude relative to the red autocorrelation amplitude is low, meaning that only a small fraction of the green-labeled protein co-localizes with the red liposomes. Although the reconstitution yield is unsatisfactory in this experiment, the size of the protein–lipid particles is as desired, as evidenced by a single component fit of the cross-correlation curve with τ_{diff} = 2.3 ms [liposomes].

Next, we tested the use of destabilized liposomes and mixed micelles in the coexistence region (1.5 mM Triton, see Fig. 2) as the starting material, to which the solubilized protein was added. The detergent was again removed by the repeated addition of Bio-Beads (7 to 10 beads per step). Clearly, in this experiment, aggregation occurred (Fig. 3B). This is obvious from the correlation functions, where in all three curves a second, slowly diffusing species with τ_{diff} above 30 ms appears (red autocorrelation: 70% of 2.2 ms [liposomes] and 30% of 43 ms [aggregates]; green autocorrelation: 60% of 1.6 ms [liposomes] and 40% of 33 ms [aggregates]; cross-correlation: 58% of 2.1 ms [liposomes] and 42% of 32 ms [aggregates]). The fact that this slowly diffusing species appears also in the cross-correlation curve shows that protein and lipid co-localize in the aggregates. The cross-correlation amplitude, which indicates co-localization of protein and lipid, is high

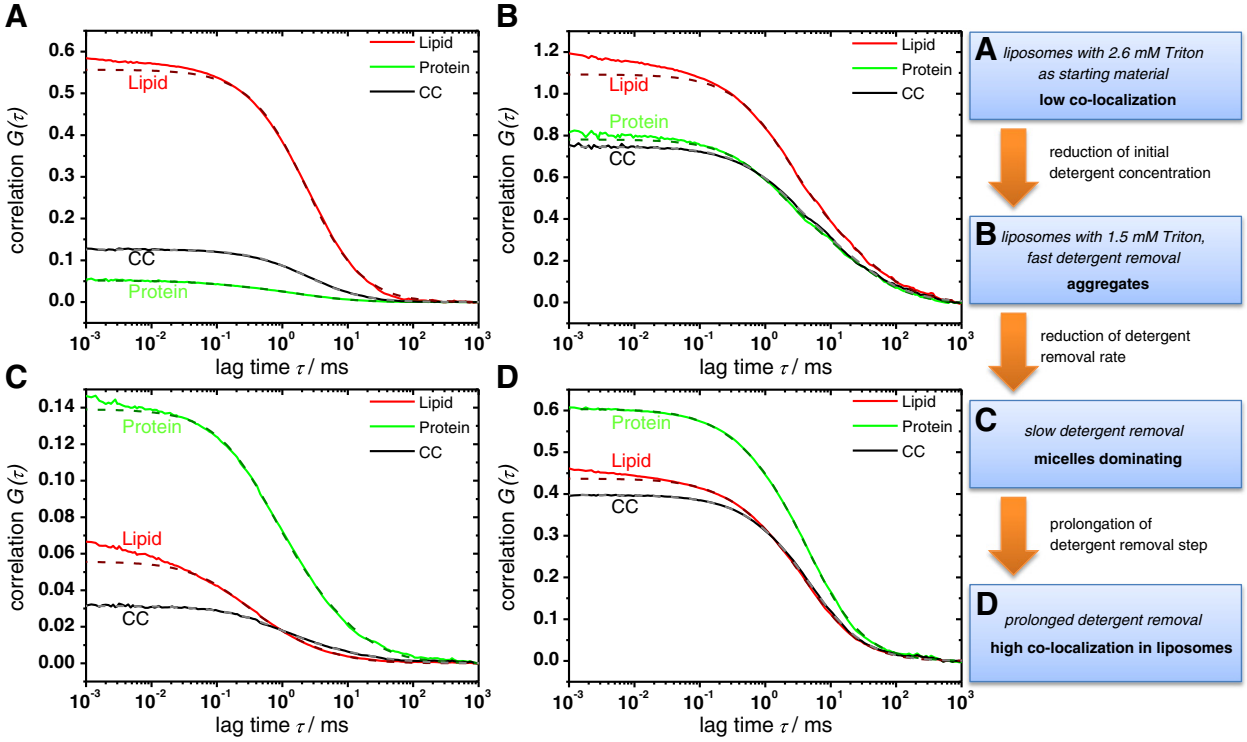

Fig. 3. Dual-color FCCS measurements monitoring and guiding the NorA-GFP reconstitution process. (A–D) FCCS measurements of samples prepared under different conditions are shown. The optimization of the reconstitution process is summarized on the right. Red denotes the lipid marker, green the fluorescent protein and black the cross-correlation. Measured FCCS curves (solid lines) were fitted using Eqs. (2) and (3). Dashed curves were calculated from the parameter fit values, without the blinking term. The dashed curves represent diffusion only, allowing a direct visual assessment of the correlation amplitudes and half-lives. See text for a detailed discussion.

in comparison with either of the autocorrelation amplitudes, corroborating that co-localization was obtained at the cost of aggregation.

We reasoned that aggregation may have been caused by an overly rapid removal of the detergent and therefore reduced the rate of addition of the Bio-Beads to 4 to 6 beads per step for the next experiment (Fig. 3C). The same starting material (1.5 mM Triton, coexistence of micelles and liposomes) was used. After a 19 hour incubation with Bio-Beads added at the slow rate, the shapes of the correlation curves still showed a large amount of micelles in the sample (red autocorrelation: 78% of 0.25 ms [micelles] and 22% of 3.3 ms [liposomes]; green autocorrelation: 73% of 0.65 ms [micelles] and 27% of 8.7 ms [aggregates]; cross-correlation: 76% of 0.85 ms [micelles] and 24% of 19 ms [aggregates]). The low absolute values of the correlation amplitudes (i.e., the large numbers of particles) in Fig. 3C in comparison with panels A, B and D also supported that the majority of material was still in the form of micelles. However, even though the sample contained micelles and aggregates, this reconstitution attempt was promising, because the micellar species was part of the cross-correlation curve, indicating the formation of mixed micelles comprising both protein and lipid. We therefore checked if extending the incubation time with Bio-Beads might lead to the formation of the desired proteoliposomes.

Fig. 3D shows the FCCS analysis of this reconstitution sample after an extension of the incubation time with Bio-Beads to 26 h. The correlation curve amplitudes provide valuable pieces of information on the sample: Firstly, the absolute values of the correlation amplitudes have increased (i.e., the number of particles has decreased), in line with the assembly of larger, liposomal particles. Secondly, the amplitude of the cross-correlation is high compared to the autocorrelation curves, demonstrating that the co-localization of NorA-GFP and lipids is dominant. Thirdly, the red autocorrelation amplitude is below the green autocorrelation amplitude, which is expected for an optimal reconstitution. The shapes of the correlation curves confirm that proteoliposomes constitute the dominating species, but also reveal remaining micelles (red autocorrelation: 22% of 0.57 ms [micelles] and 78% of 4.8 ms [liposomes]; green autocorrelation: 15% of 0.41 ms [micelles] and 85% of 4.7 ms [liposomes]; cross-correlation: 10% of 0.63 ms [micelles] and 90% of 5.1 ms [liposomes]). An incomplete sequestration of the detergent from reconstitution reactions is a known disadvantage of the use of Triton X-100 and Bio-Beads [46].

These four examples demonstrate that dual-color FCCS allows to specifically detect the co-localization of the GFP-labeled NorA protein with liposomes. Co-localization of protein and lipid in aggregates (Fig. 3B), mixed micelles (Fig. 3C) and liposomes (Fig. 3D) is distinguishable from one another by virtue of the different diffusion characteristics.

The cross-correlation between green-labeled membrane protein and red-labeled liposomes is highly sensitive to the formation of proteoliposomes on a qualitative level. However, the relative cross-correlation amplitude is rather insensitive to the exact number of proteins per liposome. Brightness analysis methods could be explored for the purpose of determining the number of proteins per liposome. For a quantitative analysis of particle brightnesses, potential brightness changes due to quenching or fluorescence resonance energy transfer will need to be considered.

3.4. Transport activity of NorA-GFP proteoliposomes

Since the co-localization of the membrane transporter NorA and the liposomes does not necessarily mean a functional reconstitution, a transport assay according to the method described by Putman et al. was used to determine the transport activity of NorA reconstituted in liposomes (Fig. 4) [47]. This assay takes advantage of the characteristic properties of Hoechst 33342 being highly fluorescent in a hydrophobic environment and not fluorescent in an aqueous environment. For liposomes lacking NorA, no significant change in Hoechst fluorescence was observed during the time course of the measurement. In contrast,

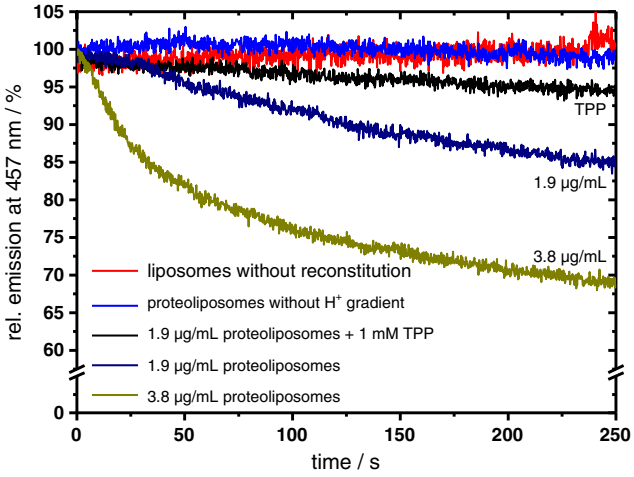

Fig. 4. Hoechst 33342 transport assay using NorA-GFP proteoliposomes. Time traces of fluorescence intensities at 457 nm (excitation wavelength 355 nm) after imposing an artificial proton gradient are shown for two different NorA-GFP proteoliposome concentrations (dark blue — 1.9 µg/mL proteoliposomes, yellow — 3.8 µg/mL proteoliposomes). Empty liposomes without reconstituted protein (red) and NorA-GFP proteoliposomes in the absence of a proton gradient (light blue) served as controls. The inhibitory effect of the competitive substrate TPP (10 µM) on Hoechst 33342 (10 µM) transport was also tested (black).

successfully reconstituted NorA-GFP proteoliposomes showed a decreasing Hoechst fluorescence signal (Fig. 4), indicating the transport of the dye from the hydrophobic membrane interior to the aqueous environment outside of the bilayer. Furthermore, doubling the proteoliposome concentration augmented the decrease in Hoechst fluorescence. The Hoechst 33342 transport activity assay was also performed in the presence of TPP, another known substrate of NorA that is structurally unrelated to Hoechst [34]. The addition of equimolar concentrations of TPP and Hoechst 33342 led to a reduced transport of the Hoechst 33342 (Fig. 4), suggesting that both compounds compete as a substrate of NorA. The results additionally demonstrate that the C-terminally-fused GFP does not interfere with the transport activity of NorA.

4. Conclusion

Exploitation of the highly sensitive and specific optical techniques FCS and dual-color FCCS provides a powerful tool for monitoring the detergent-mediated reconstitution of a membrane protein into liposomes. The reconstitution of NorA-GFP into liposomes was optimized using the particle size, particle number, fractional composition and dynamic co-localization information contained in the dual-color fluorescence correlation curves. The Hoechst transport assay confirmed functionally active NorA-proteoliposomes. This versatile approach to guide the optimization of membrane protein reconstitution can be readily applied to other membrane transporters as well as any other fluorescently tagged membrane protein.

Acknowledgment

This work was supported by the Bundesministerium für Bildung und Forschung (BMBF) ZIK program (FKZ 03Z2HN21 to M.T.; FKZ 03Z2HN22 to K.B.) and ERDF (grant 1241090001 to M.T. and K.B.). We thank Ines Jacob, Christof Kattner and Claudia Müller for experimental assistance, David Drew (Stockholm University) for providing the plasmid pWaldo-eGFP and Jochen Balbach and Milton T. Stubbs for critical reading of the manuscript.

The authors declare no conflicts of interest.

Appendix A. Supplementary data

Supplementary data to this article can be found online at http://dx.doi.org/10.1016/j.bpc.2013.08.003.

References

[1] Q. Ren, K. Chen, I.T. Paulsen, TransportDB: a comprehensive database resource for cytoplasmic membrane transport systems and outer membrane channels, Nucleic Acids Res. 35 (2007) D274–D279.
[2] J.L. Rigaud, D. Levy, Reconstitution of membrane proteins into liposomes, Methods Enzymol. 372 (2003) 65–86.
[3] J.L. Rigaud, B. Pitard, D. Levy, Reconstitution of membrane proteins into liposomes: application to energy-transducing membrane proteins, Biochim. Biophys. Acta 1231 (1995) 223–246.
[4] M.T. Paternostre, M. Roux, J.L. Rigaud, Mechanisms of membrane protein insertion into liposomes during reconstitution procedures involving the use of detergents. 1. Solubilization of large unilamellar liposomes (prepared by reverse-phase evaporation) by triton X-100, octyl glucoside, and sodium cholate, Biochemistry 27 (1988) 2668–2677.
[5] A. Helenius, K. Simons, Solubilization of membranes by detergents, Biochim. Biophys. Acta 415 (1975) 29–79.
[6] F.M. Goni, A. Alonso, Spectroscopic techniques in the study of membrane solubilization, reconstitution and permeabilization by detergents, Biochim. Biophys. Acta 1508 (2000) 51–68.
[7] D. Lichtenberg, H. Ahyayauch, A. Alonso, F.M. Goni, Detergent solubilization of lipid bilayers: a balance of driving forces, Trends Biochem. Sci. 38 (2013) 85–93.
[8] S. Almog, B.J. Litman, W. Wimley, J. Cohen, E.J. Wachtel, Y. Barenholz, A. Ben-Shaul, D. Lichtenberg, States of aggregation and phase transformations in mixtures of phosphatidylcholine and octyl glucoside, Biochemistry 29 (1990) 4582–4592.
[9] M.L. Jackson, C.F. Schmidt, D. Lichtenberg, B.J. Litman, A.D. Albert, Solubilization of phosphatidylcholine bilayers by octyl glucoside, Biochemistry 21 (1982) 4576–4582.
[10] F.M. Goni, M.A. Urbaneja, J.L. Arrondo, A. Alonso, A.A. Durrani, D. Chapman, The interaction of phosphatidylcholine bilayers with Triton X-100, Eur. J. Biochem. 160 (1986) 659–665.
[11] D. Levy, A. Bluzat, M. Seigneuret, J.L. Rigaud, A systematic study of liposome and proteoliposome reconstitution involving Bio-Bead-mediated Triton X-100 removal, Biochim. Biophys. Acta 1025 (1990) 179–190.
[12] D. Lichtenberg, Y. Zilberman, P. Greenzaid, S. Zamir, Structural and kinetic studies on the solubilization of lecithin by sodium deoxycholate, Biochemistry 18 (1979) 3517–3525.
[13] E. London, G.W. Feigenson, Phosphorus NMR analysis of phospholipids in detergents, J. Lipid Res. 20 (1979) 408–412.
[14] J.L. Arrondo, F.M. Goni, Infrared studies of protein-induced perturbation of lipids in lipoproteins and membranes, Chem. Phys. Lipids 96 (1998) 53–68.
[15] J.L. Arrondo, F.M. Goni, Structure and dynamics of membrane proteins as studied by infrared spectroscopy, Prog. Biophys. Mol. Biol. 72 (1999) 367–405.
[16] A. Alonso, R. Saez, F.M. Goni, The interaction of detergents with phospholipid vesicles: a spectrofluorimetric study, FEBS Lett. 137 (1982) 141–145.
[17] W.J. Degrip, J. Vanoostrum, P.H. Bovee-Geurts, Selective detergent-extraction from mixed detergent/lipid/protein micelles, using cyclodextrin inclusion compounds: a novel generic approach for the preparation of proteoliposomes, Biochem. J. 330 (1998) 667–674.
[18] O. Eidelman, R. Blumenthal, A. Walter, Composition of octyl glucoside–phosphatidylcholine mixed micelles, Biochemistry 27 (1988) 2839–2846.
[19] M. Ollivon, O. Eidelman, R. Blumenthal, A. Walter, Micelle–vesicle transition of egg phosphatidylcholine and octylglucoside, Biochemistry 27 (1988) 1695–1703.
[20] H. Heerklotz, J. Seelig, Titration calorimetry of surfactant–membrane partitioning and membrane solubilization, Biochim. Biophys. Acta 1508 (2000) 69–85.
[21] E. Opatowski, D. Lichtenberg, M.M. Kozlov, The heat of transfer of lipid and surfactant from vesicles into micelles in mixtures of phospholipid and surfactant, Biophys. J. 73 (1997) 1458–1467.
[22] D. Marsh, A. Watts, R.D. Pates, R. Uhl, P.F. Knowles, M. Esmann, ESR spin-label studies of lipid–protein interactions in membranes, Biophys. J. 37 (1982) 265–274.
[23] B. Angelov, M. Ollivon, A. Angelova, X-ray diffraction study of the effect of the detergent octyl glucoside on the structure of lamellar and nonlamellar lipid/water phases of use for membrane protein reconstitution, Langmuir 15 (1999) 8225–8234.
[24] S. Morandat, K. El Kirat, Membrane resistance to Triton X-100 explored by real-time atomic force microscopy, Langmuir 22 (2006) 5786–5791.
[25] S. Morandat, K. El Kirat, Solubilization of supported lipid membranes by octyl glucoside observed by time-lapse atomic force microscopy, Colloids Surf. B: Biointerfaces 55 (2007) 179–184.
[26] M. Almgren, Mixed micelles and other structures in the solubilization of bilayer lipid membranes by surfactants, Biochim. Biophys. Acta 1508 (2000) 146–163.
[27] P.K. Vinson, Y. Talmon, A. Walter, Vesicle–micelle transition of phosphatidylcholine and octyl glucoside elucidated by cryo-transmission electron microscopy, Biophys. J. 56 (1989) 669–681.
[28] A. Walter, P.K. Vinson, A. Kaplun, Y. Talmon, Intermediate structures in the cholate-phosphatidylcholine vesicle–micelle transition, Biophys. J. 60 (1991) 1315–1325.
[29] R. Rigler, E.S. Elson, Fluorescence Correlation Spectroscopy: Theory and Applications, 1st ed. Springer, New York, 2001.
[30] K. Bacia, P. Schwille, Practical guidelines for dual-color fluorescence cross-correlation spectroscopy, Nat. Protoc. 2 (2007) 2842–2856.
[31] H. Yoshida, M. Bogaki, S. Nakamura, K. Ubukata, M. Konno, Nucleotide sequence and characterization of the *Staphylococcus aureus* norA gene, which confers resistance to quinolones, J. Bacteriol. 172 (1990) 6942–6949.
[32] I.T. Paulsen, M.H. Brown, R.A. Skurray, Proton-dependent multidrug efflux systems, Microbiol. Rev. 60 (1996) 575–608.
[33] P.C. Hsieh, S.A. Siegel, B. Rogers, D. Davis, K. Lewis, Bacteria lacking a multidrug pump: a sensitive tool for drug discovery, Proc. Natl. Acad. Sci. U. S. A. 95 (1998) 6602–6606.
[34] A.A. Neyfakh, C.M. Borsch, G.W. Kaatz, Fluoroquinolone resistance protein NorA of *Staphylococcus aureus* is a multidrug efflux transporter, Antimicrob. Agents Chemother. 37 (1993) 128–129.
[35] J.L. Yu, L. Grinius, D.C. Hooper, NorA functions as a multidrug efflux protein in both cytoplasmic membrane vesicles and reconstituted proteoliposomes, J. Bacteriol. 184 (2002) 1370–1377.
[36] D.E. Drew, G. von Heijne, P. Nordlund, J.W. de Gier, Green fluorescent protein as an indicator to monitor membrane protein overexpression in *Escherichia coli*, FEBS Lett. 507 (2001) 220–224.
[37] J.D. Pedelacq, S. Cabantous, T. Tran, T.C. Terwilliger, G.S. Waldo, Engineering and characterization of a superfolder green fluorescent protein, Nat. Biotechnol. 24 (2006) 79–88.
[38] D. Drew, M. Lerch, E. Kunji, D.J. Slotboom, J.W. de Gier, Optimization of membrane protein overexpression and purification using GFP fusions, Nat. Methods 3 (2006) 303–313.
[39] J. Knol, K. Sjollema, B. Poolman, Detergent-mediated reconstitution of membrane proteins, Biochemistry 37 (1998) 16410–16415.
[40] M.D. Womack, D.A. Kendall, R.C. MacDonald, Detergent effects on enzyme activity and solubilization of lipid bilayer membranes, Biochim. Biophys. Acta 733 (1983) 210–215.
[41] P.W. Holloway, A simple procedure for removal of Triton X-100 from protein samples, Anal. Biochem. 53 (1973) 304–308.
[42] Z. Petrasek, P. Schwille, Precise measurement of diffusion coefficients using scanning fluorescence correlation spectroscopy, Biophys. J. 94 (2008) 1437–1448.
[43] A. Loman, C.B. Müller, F. Koberling, W. Richtering, J. Enderlein, Absolute and precise measurement of the diffusion of small fluorescent dye molecules across the visible spectrum, 14th International Workshop on Single Molecule Spectroscopy and Ultrasensitive Analysis in Life Science, Poster, Berlin, Germany, 2008.
[44] J. Sot, M.I. Collado, J.L.R. Arrondo, A. Alonso, F.M. Goñi, Triton X-100-resistant bilayers: effect of lipid composition and relevance to the raft phenomenon, Langmuir 18 (2002) 2828–2835.
[45] A. Alonso, M.A. Urbaneja, F.M. Goni, F.G. Carmona, F.G. Canovas, J.C. Gomez-Fernandez, Kinetic studies on the interaction of phosphatidylcholine liposomes with Triton X-100, Biochim. Biophys. Acta 902 (1987) 237–246.
[46] J.L. Rigaud, D. Levy, G. Mosser, O. Lambert, Detergent removal by non-polar polystyrene beads, Eur. Biophys. J. 27 (1998) 305–319.
[47] M. Putman, H.W. van Veen, B. Poolman, W.N. Konings, Restrictive use of detergents in the functional reconstitution of the secondary multidrug transporter LmrP, Biochemistry 38 (1999) 1002–1008.